Properties of the Al-Si solid solution: Dynamical properties of the silicon substitutional and the aluminum vacancy

A. Caro*
Paul Scherrer Institute, 5232 - Villigen PSI, Switzerland

D. A. Drabold
Department of Physics and Astronomy, Condensed Matter and Surface Sciences Program, Ohio University, Athens, Ohio 45701

O. F. Sankey
Department of Physics and Astronomy, Arizona State University, Tempe, Arizona 85287
(Received 2 August 1993)

Using *ab initio* total-energy and molecular dynamics based on local orbitals and density-functional theory, we present results on the nonequilibrium Al-Si solid solution. We report on relaxations, vibrational spectrum, and superconducting transition temperature. Our results are in excellent agreement with experimental measurements on rapidly quenched samples which show evidence of lattice instabilities induced by the solute. We perform a similar analysis on the vibrational properties of the Al vacancy and discuss the results in terms of the mechanical instability leading to the crystalline-to-amorphous transition.

I. INTRODUCTION

Metals like sodium, magnesium, and aluminum are the simplest form of condensed matter. They crystallize in close-packed structures and their electrons behave as free particles weakly perturbed by the presence of the ions. Because of the elementary electronic structure, the problem of defects in these simple metals has been for a long time a benchmark for theoretical approaches. In fact most of the calculation techniques, starting from the simple pair potentials to the most complex first-principles theories, have been applied to them.

At the early times, pseudopotentials and perturbation theory in the linear-response approach were supposed to give a good description of their electronic structure. This lead to the development of pair potentials plus volume terms, an approach widely used for many years to study defects in most metals.[1-3] It soon appeared that this approach was inadequate for polyvalent metals with high electronic density like Al, because of nonlinear effects that, if neglected, give unrealistic defect energetics, for example vacancy-formation energies close to zero.[4,5] Higher-order perturbations did not provide a conclusive result.[6]

This situation changed some years ago due to important progress made in two main directions: On one side, a semiempirical method, known as the embedded-atom model,[7,8] replaced the pair potential plus volume term, by a many-body potential derived from tight-binding or density-functional theories (DFT). This had great success for the late transition metals, although the situation was less satisfactory for simple metals.[9-11] On the other side, recent substantial progress in full *ab initio* calculations made it possible to deal with such large-scale problems on a first-principles basis.[12,13] Also relevant to mention are those models developed between these two approaches, namely the tight-binding or one electron picture of the chemical bonding, also applied to Al.[14]

With these tools now at hand, many matrix-solute combinations can be accurately described, in addition to intrinsic point defects. A very attractive problem is silicon as substitutional impurity in aluminum, as it induces dramatic effects on many physical properties, indicating a possible way to amorphize via a mechanical instability.[15-17] At room temperature Al and Si are two immiscible elements; the Si solubility at 550 K is only 0.05%. The AlSi alloys close to equilibrium are composed of two distinct phases, fcc metallic Al, and Si in the diamond structure. Attempts to stabilize the solid solution by standard rapid quenching from the melt lead to the presence of small Si precipitates, with strong effects on the superconducting transition temperature (from 1.1 K for pure Al to 11 K for Al 18% Si).[18] In the last few years, a new technique of quenching under high pressure was applied by Chevrier and co-workers to produce homogeneous solid solutions for Si concentrations up to 10%.[19-22] Pressures in the range of 50 kBar and temperatures of 1000 K significantly increase the solubility because of the tendency of Si to become metallic; at about 100 kBar pure Si transforms into a metallic β-Sn compact structure whose volume per atom (15.5 Å^3) is much closer to Al (16.6 Å^3) than to covalent Si (20 Å^3). Quenching rates of 100 K/sec under pressure retain the Si atoms trapped at substitutional Al sites.

These samples show important changes in several properties, namely, (a) a significant decrease of the lattice parameter of the fcc matrix: -0.35% for 6% Si, (b) a significant increase of the superconducting transition temperature, from 1.1 K for pure Al to 4.4 K for Al 10% Si, (c) a large modification of the phonon density of states

(DOS) implying a decrease of the Debye temperature, also a decrease of the shear modulus (up to 35% for Al 10% Si); (d) the presence of an abnormal linear term in the low-temperature specific heat, similar to what is observed in amorphous samples exhibiting two-level system excitations; and (e) an important exothermal reaction under annealing at high temperature, giving a heat of dissolution under normal pressure equal to 38 kJ/mol.

Although the lowest concentration experimentally studied is 4% Si, in the analysis of the results it is assumed that these effects are due to local dynamical properties of a single impurity. Recent measurements on such properties on other systems indicate a large softening of the host matrix around the impurity. In PbSn solid solution, for example, the change of the Pb dynamics around a Sn impurity is so large that the authors describe it as a local melting.[23,24]

These observations lead the authors in Refs. 19–22 to conclude that the nonequilibrium AlSi solid solutions behave, with respect to pure Al, in a manner like amorphous metallic alloys, with the important difference that AlSi is still crystalline. The question of whether the lattice instability induced by Si may lead to a massive amorphization at higher concentrations is however still open.

The purpose of this work is to calculate the dynamical properties of substitutional Si in Al and to compare with the dynamics of the Al vacancy, to find similarities in the behavior of both defects. We use *ab initio* molecular dynamics (MD), based on density-functional theory (DFT), on cells large enough to determine the relaxations around the defects.

II. METHOD OF CALCULATION

Sankey and Niklewski have recently developed an approximate first-principles electronic structure method that closely matches a more rigorous calculation, but greatly reduces the computational effort required.[13] We employ this *ab initio* local orbital density-functional MD scheme which is very well documented and proven. We refer the reader to the literature[25] for tests and applications. The essential approximations are (1) Nonlocal, norm conserving pseudopotentials of the Hamann-Schlüter-Chiang type;[26] (2) a set of four local orbitals per site with confinement boundary conditions[13] (the confinement radii are 6 and 5 Bohr radii, for Al and Si, respectively); and (3) the method uses the Harris functional implementation of the local-density approximation (LDA),[27] assuming a spin unpolarized system with doubly occupied orbitals. The exchange-correlation functional is assumed to be of the Ceperley-Alder form, as parametrized by Perdew and Zunger.[28,29] Forces were determined using the Hellman-Feynman theorem as discussed in Ref. 13.

In this work we use a supercell of 107 Al atoms arranged in an fcc lattice with periodic boundary conditions, and a vacancy or a Si atom at its center. The electronic structure is calculated with four special points in the Brillouin zone. The defects are first allowed to relax by the steepest descent algorithm, until all forces are less than 0.01 eV/Å. The vibrational properties are obtained from the diagonalization of the dynamical matrix $\Phi^{ij}_{\alpha\beta}$, which in turn is obtained from the forces acting on atom j direction β when atom i is moved 0.03 Å in the direction α.

III. RESULTS

A. AlSi solid solution

Lattice relaxations

Lattice relaxations around Si are significant, as reported in Table I and fig. 1. They are all inwards, with a maximum of -2.8% at the first layer. An oscillatory pattern develops, although without a change in sign in the magnitude of the relaxations; we come back to this point later. With our calculation being made at constant volume, we are unable to determine the volume contraction upon the creation of such a substitutional defect; we can only assert that there is a volume contraction, compatible with the experimental observations.[20]

Dynamics

To analyze the vibrational properties of the defect lattice we study the participation ratio of the modes, which reflects the number of sites that participate on a given mode:

$$P_r = \Sigma_\alpha \varphi_\alpha^2 / \Sigma_\alpha \varphi_\alpha^4 , \quad (1)$$

where α denotes the vibrational eigenmode and φ_α the corresponding eigenvector. In Figs. 2 and 3 we report the participation ratio P_r, Eq. (1), and the amplitude of modes at the Si atom, respectively. A clear, although weak, tendency to localization on the impurity of some low- and high-energy modes comes out from these figures. It is important to point out that the cell size $(3\times3\times3)a_0^3$, with a_0 the lattice parameter, and the way we determine the spectrum (Γ point for phonons) imply a low-frequency cutoff of about 100 cm^{-1}.

We have identified some of the modes appearing with high weight on the Si atom. Considering for simplicity only the subspace formed by the Si substitutional and its 12 nearest neighbors (nn) using the cubic symmetry, and noting that from the 36 modes of the 12 nn, only three involve motion of the center of mass and can then couple to the Si impurity, it turns out that a total of four eigenmodes include Si. For a longitudinal spring model, three out of these four modes have zero frequency because they involve only transverse relative displacements, and the

TABLE I. Lattice relaxations.

Shell	Al vacancy	Si substitutional
⟨1st⟩	−0.011 Å (−0.38%)	−0.08 Å (−2.8%)
⟨2nd⟩	0.010 Å (0.25%)	−0.026 Å (−0.66%)
⟨3rd⟩	0.014 Å (0.28%)	−0.051 Å (−1.08%)
⟨4th⟩	0.002 Å (0.03%)	−0.055 Å (−0.97%)
⟨5th⟩	0.004 Å (0.06%)	−0.013 Å (−0.2%)

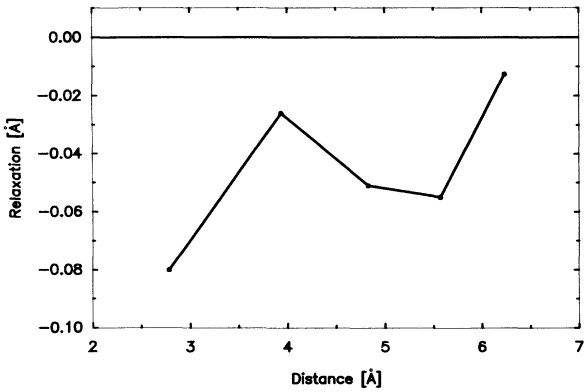

FIG. 1. Lattice relaxations of the first five shells around a Si substitutional impurity in the Al matrix.

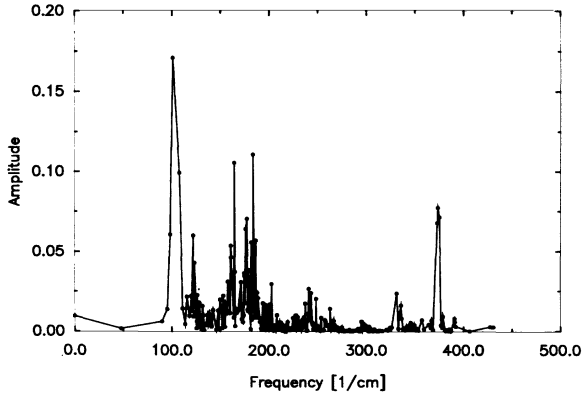

FIG. 3. Amplitude of the eigenmodes projected on the Si atom. Modes with high amplitude are discussed in the text.

fourth has a high eigenvalue (for a detailed discussion see Ref. 30). Our calculation gives several eigenstates with large amplitude on the Si atoms, as reported in Fig. 3. The three high-frequency modes around 375 cm^{-1} correspond to motion of the Si atom pointing to a nn which itself moves towards the Si atom, or motion of Si towards the center of the square formed by four nn, who move against Si. Similarly the low-frequency modes analyzed at around 100 cm^{-1} correspond to in-phase motion of Si and its nn along (110) or (100) directions; all these modes have a large component on the basic eigenmodes of the 12+1 substitutional of cubic symmetry discussed above. It can be concluded that the local spectrum is well characterized by the standard analysis in terms of the properties of a cubic substitutional characterized by coupling constants weaker than those of the matrix.

The local density of vibrational states at the Si site is shown in Fig. 4. These spectra, and all those shown in this paper, are obtained from the eigenvalues using a Lorentzian of width 30 cm^{-1}, to match the experimental resolution of the neutron spectrometer used in Refs. 20 and 22. Three nonequivalent directions, namely (110), (111), and (001), show a remarkable isotropy, with the main result being a substantial softening of the frequencies, much larger than what is expected from the mass ratio $M/M_0=1.04$, indicating a significant decrease in the coupling constants. Similar behavior is observed at the nearest neighbors (nn) and second-nearest neighbors (nnn) located at $a_0/2$ (110) and a_0 (100), Figs. 5 and 6, respectively. In these last figures, once again we report three nonequivalent directions adapted to the symmetry of the particular site, and we conclude that motion pointing to the Si impurity, along (110) for nn, and along (100) for nnn, are softer than in other directions, revealing the weak coupling to Si. Also interesting is the shift of the upper band edge towards higher frequencies in the case of (001) displacements, as seen in Fig. 5.

The DOS at the nnn is still quite different from the perfect crystal DOS reported in Fig. 7, indicating the long range of the perturbation. Summing the LDOS for all atoms in the cell, we obtain the total DOS reported in Fig. 7. This figure has to be compared with the experimental results of Ref. 20. The agreement in the main features of the spectrum between our results for 1% Si concentration and the experiments for 4% is extremely good.

It is instructive to trace out the origin of these features by inspecting the dynamical matrix $\Phi^{ij}_{\alpha\beta}=\psi^{ij}_{\alpha\beta}/(M^{i*}M^{j})^{1/2}$, where $\psi^{ij}_{\alpha\beta}$ is the force constant ma-

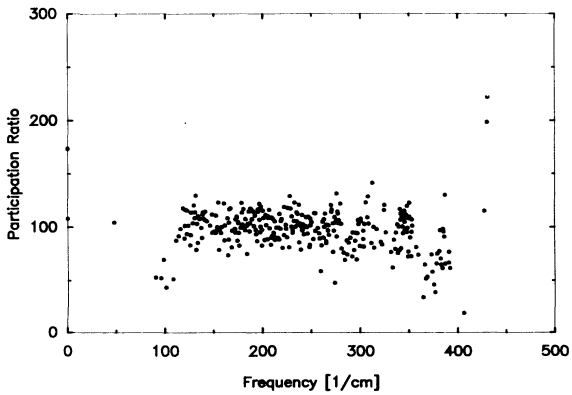

FIG. 2. Participation ratio P_r, Eq. (1), of the eigenmodes of the supercell containing 107 Al atoms and the Si impurity. A tendency towards localization of some low- and high-frequency modes is observed.

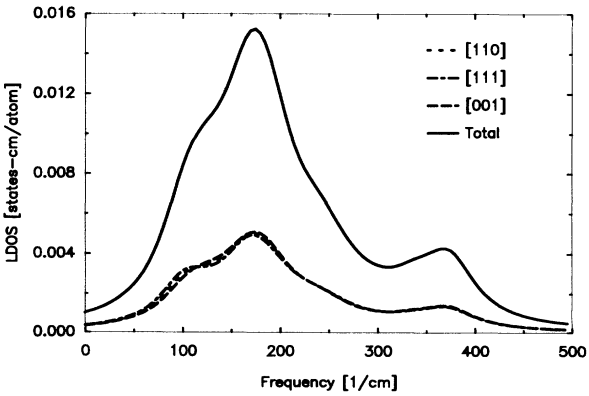

FIG. 4. Local density of states (LDOS) on the Si impurity. Three partial LDOS along nonequivalent directions are reported, together with the total LDOS. A significant softening with respect to the perfect lattice, Fig. 7, is observed.

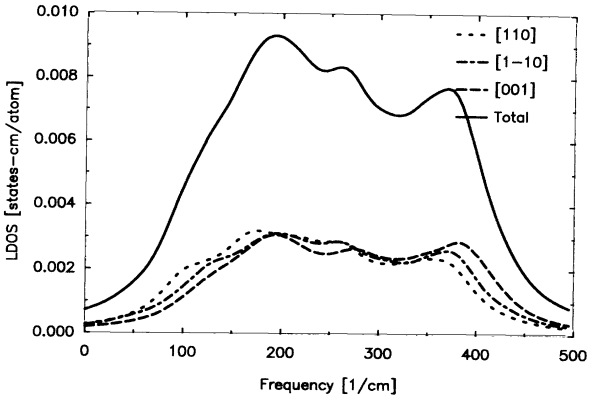

FIG. 5. Local density of states (LDOS) on the Al atom located at $a_0/2$ (110), nearest neighbor to the Si impurity at the origin. Three partial LDOS along nonequivalent directions are reported, together with the total LDOS.

trix. Let us first analyze the diagonal matrix corresponding to the Si atom, that we denote by Φ^{000} (with the superscript indicating the difference $\mathbf{r}_j-\mathbf{r}_i$), and those relating it to its nn, $\Phi^{1/2\,1/2\,0}$, and nnn, Φ^{100}:

$$\Phi^{0,0,0}=\begin{matrix}0.17 & 0.0 & 0.0\\ 0.0 & 0.17 & 0.0\\ 0.0 & 0.0 & 0.17\end{matrix},$$

$$\Phi^{1/2,1/2,0}=\begin{matrix}-0.03 & -0.03 & 0.0\\ -0.03 & -0.03 & 0.0\\ 0.0 & 0.0 & 0.01\end{matrix},$$

$$\Phi^{1,0,0}=\begin{matrix}-0.01 & 0.0 & 0.0\\ 0.0 & -0.01 & 0.0\\ 0.0 & 0.0 & -0.01\end{matrix},$$

and compare with the perfect crystal case, that with denote with the subscript Φ_0:

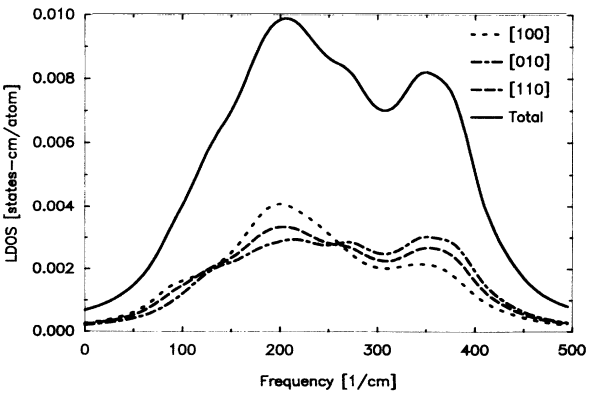

FIG. 6. Local density of states (LDOS) on the Al atom located at a_0 (100), second-nearest neighbor to the Si impurity at the origin. Three partial LDOS along nonequivalent directions are reported, together with the total LDOS.

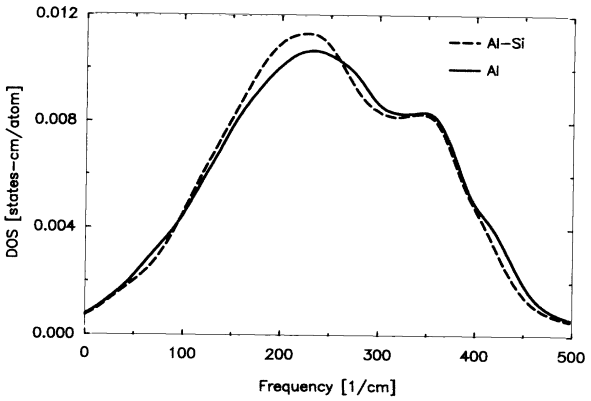

FIG. 7. Total LDOS of the 108 atom supercells, for pure Al and 107 Al plus 1 Si, making an atomic concentration of $\approx 1\%$.

$$\Phi_0^{0,0,0}=\begin{matrix}0.24 & 0.0 & 0.0\\ 0.0 & 0.24 & 0.0\\ 0.0 & 0 & 0.24\end{matrix},$$

$$\Phi_0^{1/2,1/2,0}=\begin{matrix}-0.04 & -0.02 & 0.0\\ -0.02 & -0.04 & 0.0\\ 0.0 & 0.0 & 0.01\end{matrix},$$

$$\Phi_0^{1,0,0}=\begin{matrix}0.02 & 0.0 & 0.0\\ 0.0 & 0.02 & 0.0\\ 0.0 & 0.0 & 0.02\end{matrix},$$

These matrix elements are given in units of eV/(Å amu), {the factor transforming $[\text{eV}/(\text{Å emu})]^{1/2}$ into cm^{-1} is 519.6.}.

From Φ_0^{000} and Φ^{000} we see that the Einstein frequency of Si is 18% less than that of Al: 210 $\text{cm}:^{-1}$ versus 255 cm^{-1}, respectively. The interaction between nearest neighbors, located at $a_0/2$ (110) and a_0 (100), analyzed in terms of longitudinal and transverse couplings $\Phi_=$ and $\Phi_\perp$,

$$\Phi_=^{1,1,0}=\{[(\Phi^{1/2,1/2,0})_{xx}+(\Phi^{1/2,1/2,0})_{yx}]^2 + [\Phi^{1/2,1/2,0})_{xy}+(\Phi^{1/2,1/2,0})_{yy}]^2\}^{1/2},$$

$$\Phi_\perp^{1,1,0}=\{[(\Phi^{1/2,1/2,0})_{xx}-(\Phi^{1/2,1/2,0})_{yx}]^2 - [\Phi^{1/2,1/2,0})_{xy}+(\Phi^{1/2,1/2,0})_{yy}]^2\}^{1/2}$$

show a similar longitudinal spring for both pure Al and AlSi [-0.085 eV/(Å amu)] but, while in pure Al the transverse spring has a strength of -0.03 eV/(Å amu), in AlSi this interaction is zero or very small. Second neighbors show a softening of the longitudinal force constant in AlSi as compared to Al, together with a change in sign [from 0.02 eV/(Å emu)] in Al-Al to -0.01 eV/(Å emu)] for Si-Al.

It is interesting to note that these results indicate that in pure Al the pair interaction is attractive for nn and repulsive for nnn, which is not the usual behavior for an effective pair potential with a single minimum, but is in agreement with the effective pair potential for Al derived

by Harrison which contains several oscillations.[1] Also, it agrees with unpublished work of Ercolessi.[31] For Si in turn, nn and nnn interactions are attractive, as can also be qualitatively deduced from the relaxations reported in Fig. 1.

Also instructive is the analysis of the diagonal matrices corresponding to the nn and a nnn located at the same position as before:

$$\Phi_{nn}^{0,0,0}=\begin{matrix}0.25 & -0.01 & 0.0\\ -0.01 & 0.25 & 0.0\\ 0.0 & 0.0 & 0.30,\end{matrix}$$

$$\Phi_{nnn}^{0,0,0}=\begin{matrix}0.23 & 0.0 & -0.01\\ 0.0 & 0.29 & -0.01\\ -0.01 & -0.01 & 0.29.\end{matrix}$$

From Φ_{nn}^{000} it can be seen that motion along (110), pointing to the Si substitutional has the same restoring force as in a perfect crystal [0.34 eV/(Å amu)], while along (1-10) and (001) forces are harder [0.37 eV/(Å amu)]. Interesting is the fact that the transverse coupling along (001) between Al and Si, $(\Phi^{1/2,1/2,0})_{zz}$, is essentially the same as in the Al-Al interaction $(\Phi_0^{1/2,1/2,0})_{zz}$, namely 0.01 eV/(Å amu), while the total restoring force along (001) of the nearest neighbor, $(\Phi_{nn}^{000})_{zz}=0.30$ eV/(Å amu), is larger than the perfect crystal case $(\Phi_0^{000})_{zz}=0.24$ eV/(Å amu), reflecting that the hardening of the z motion of the Al atom nn to Si is not due to a direct Al-Si interaction, but rather to the complex many-body character of the interactions. As shown in Figs. 5 and 6, these features clearly show up in the local spectra.

Once again, it is important to stress the following: On one side, frequencies below 100 cm^{-1} (12 meV) are absent in our results because of size effects; the tails observed in our figures correspond to the Lorentzians; on the other side, the experiments are also unable to determine the low-frequency part of the spectrum (below 12 meV) because the presence of the elastic peak;[20] they fill that part of the spectra with second-order polynomials. Having this remark in mind, we conclude that the main influence of the presence of Si in solid solution in the Al matrix is a shift of the transverse phonon peak towards lower frequencies, together with a general, small shift of the high-frequency longitudinal phonon peak.

Figure 8 shows the difference between the perfect crystal and the 1% solid solution density of states, ΔDOS, which is to be compared with the experiment, Fig. 3 in Ref. 20. The similarity is remarkable.

From these ΔDOS all thermodynamic properties can, in principle, be obtained. However some limitations prevent us from doing so: specific heat at low temperature and Debye temperature calculations need a precise description of low-frequency modes; entropy calculations need a much larger cell to include the slow $1/r$ decrease of the shell-by-shell contribution.

A characteristic that depends on an integral property of the phonon DOS is the superconducting transition temperature. Within the framework of the McMillan analysis,[32] and assuming that the electronic properties of Al 1% Si are unchanged with respect to pure Al (the electronic density of states, extracted from the linear term in the specific heat, shows a very small variation with Si concentration[22]), the superconducting transition temperature depends on phonon properties according to

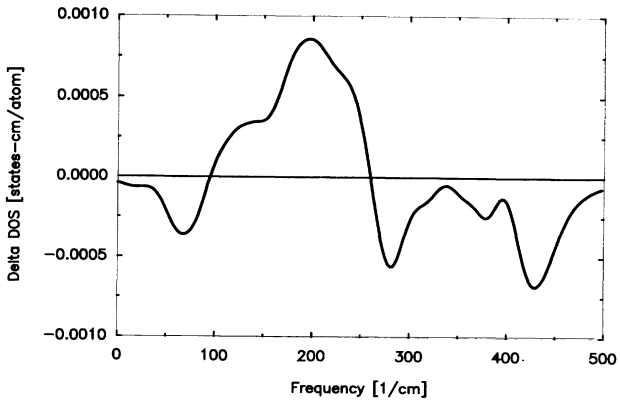

FIG. 8. Difference between the impurity cell and perfect crystal cell DOS.

$$T_c=\frac{\langle\omega\rangle}{0.595}\exp\left[\frac{1.04(1+\lambda)}{\lambda-\mu(1+0.62\lambda)}\right],$$

in this expression we have used $\langle\omega\rangle$, the average phonon frequency, as suggested in McMillans's paper, instead of the Debye temperature; λ is the electron-phonon coupling term, inversely proportional to $\langle\omega^2\rangle$, and μ is the Coulomb term. In Table II we give the values used for Al as well as our determinations of $\langle\omega\rangle$ and $\langle\omega^2\rangle$ and the predicted value of T_c (1.31 K). This increase of 20% in T_c is in excellent agreement with the experimental determinations.[19]

Our calculations, and the experimental results as well, show that Si, being smaller than Al, and having very small transverse couplings to its neighbors, destabilizes the crystalline lattice, inducing a dramatic phonon softening and a decrease of the transverse elastic constants. These features have been compared in Refs. 19–22 to the mechanisms of lattice instabilities leading to crystalline-to-amorphous transitions, and speculations concerning the critical Si concentration for such transitions to happen have also been given.[22] We can also speculate that the simplest case of a decrease of both transverse and longitudinal couplings is obtained by replacing Si by an Al vacancy.

It is experimentally unfeasible to obtain a high enough concentration of vacancies to induce an instability in Al. To learn more about the nature of such an instability, we

TABLE II. Parameters for McMillan formula.

	Al	Al 1% Si
λ	0.38	0.392
μ	0.1	0.1
$\langle\omega\rangle$ [cm^{-1}]	161.7	159.4
$\langle\omega^2\rangle$ [cm^{-2}]	47 225.3	45 746.0
T_c [K]	1.1	1.31

consider the properties of the Al vacancy, which is an even stronger perturbation than the Si substitutional.

B. Al vacancy

There are several recent papers on the Al vacancy using *ab initio* calculations; by Guillan,[33] by Jansen and Klein,[34] and Mehl and Klein,[35] and by Benedek *et al.*[36] Due to the size of the calculations, the defect has usually been studied in very small cells (up to 32 sites) that prevent a detailed description of the relaxations. Such is the case in Refs. 33 and 34, whereas in Refs. 35 and 36 a relaxation of the first shell was performed. As far as we are aware, there is no report on the dynamical properties of the Al vacancy based on results of first-principles calculations. This is the aim of this section.

Lattice relaxations

Lattice relaxations around the vacancy in Al are extremely small, less that 0.5% of the lattice spacing. Table I and Fig. 9 show the relaxations in Å of the first five shells around it. The characteristic behavior already observed for substitutional Si is the oscillatory pattern including, in this case, a change in sign. The first shell relaxes inwards by -0.011 Å, which is the same result obtained by Benedek *et al.*[36] using full self-consistent LDA and plane waves in a smaller cell (32 atoms), and is also coincident with the LAPW calculations of Mehl and Klein.[35] The size of our simulation cell allows us to analyze up to the fifth shell (the fifth shell is only partially contained in the 108 atoms supercell, therefore this value has to be considered with caution): Second and further shell relaxations are positive. The energy involved in the relaxation is small, less than 10% of the defect formation energy.[36] The oscillatory character of the relaxations around the vacancy was predicted long ago from the oscillations of the effective pair potentials derived from pseudopotential calculations.

Dynamics

A standard reference for the vibrational properties of the vacancy in fcc Cu and bcc Fe is the work by Hatcher, Zeller, and Dederich using pair potentials.[37] They determined the formation entropy and the temperature-independent part of the diffusion constant. From this work, the qualitative behavior of fcc lattices was extracted.

To analyze the vibrational properties of the Al vacancy we again study the participation ratio P_r, Eq. (1), which gives the number of sites that participate on a given mode. Figure 10 shows this parameter for all the eigenmodes, versus the eigenenergies. Some of the modes have a P_r less than 50 and may suggest a localization of the vibration. The situation in this case is however less evident than it was for Si, because we are projecting on neighbors to the defect instead of the defect itself. Many modes show a tendency to become localized around the vacancy, as can also be seen in the projected amplitudes, Fig. 11, creating a quasiresonant peak[30] in the local DOS of a nearest neighbor, Fig. 12, which shows the LDOS on atom at $a_0/2$ (110), along (110), (1-10), and (001) directions.

As expected, the main difference appears for vibrations along the direction pointing to the vacancy, where the spectrum is significantly shifted to lower frequencies. This can be intuitively understood in terms of the missing bond to the vacancy. The other two directions show a complementary effect, i.e., a shift to higher frequencies, which cannot so easily be understood in terms of the arguments used in Ref. 37 based on changes of relative distances induced by the relaxations, and consequently changes in coupling strength, since an increased strength of the nn bond is not expected: The distance between them in this direction is only slightly modified by the relaxations, and it happens in the opposite sense (increased by 0.25%).

Some relevant components of the dynamical matrix are the following: diagonal matrices of an atom nn to the vacancy, Φ_{nn}^{000} [at position $a_0/2$ (110)], of an atom nnn to the vacancy, Φ_{nnn}^{000} [at position a_0 (100)], and the nn matrix linking them $\Phi^{1/2\,-1/2\,0}$:

$$\Phi_{nn}^{0,0,0} = \begin{matrix} 0.25 & -0.05 & 0.0 \\ -0.05 & 0.25 & 0.0 \\ 0.0 & 0.0 & 0.28, \end{matrix}$$

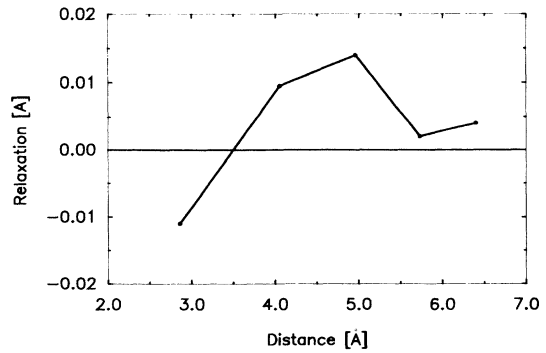

FIG. 9. Lattice relaxations of the first five shells around a vacancy in the Al matrix.

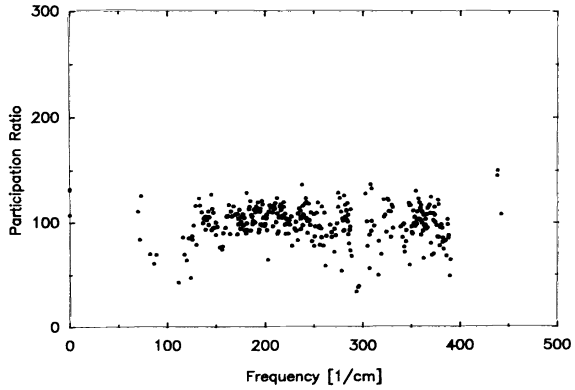

FIG. 10. Participation ratio P_r, Eq. (1), of the eigenmodes of the supercell containing 107 Al atoms and the vacancy. A tendency towards localization of some low- and high-frequency modes is observed.

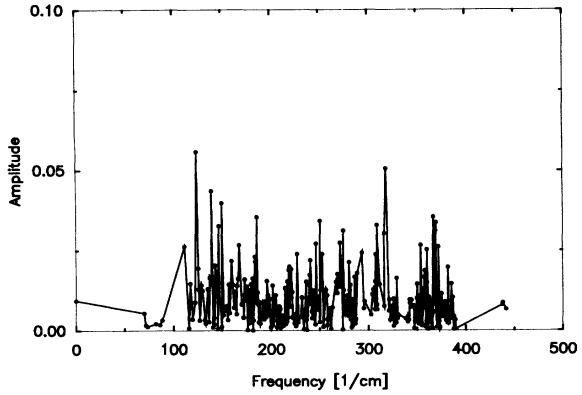

FIG. 11. Amplitude of the eigenmodes projected on an Al atom nearest neighbor to the vacancy.

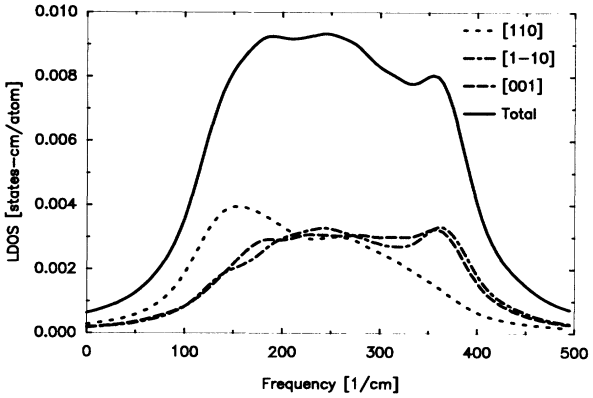

FIG. 12. Local density of states (LDOS) on the Al atom located at $a_0/2$ (110), nearest neighbor to the vacancy at the origin. Three partial LDOS along nonequivalent directions are reported, together with the total LDOS.

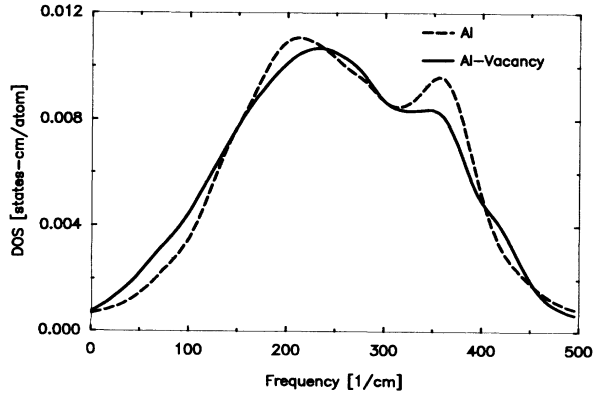

FIG. 13. Total DOS of the 108 atom supercell, for pure Al and 107 Al plus a vacancy, making an atomic concentration of $\approx 1\%$.

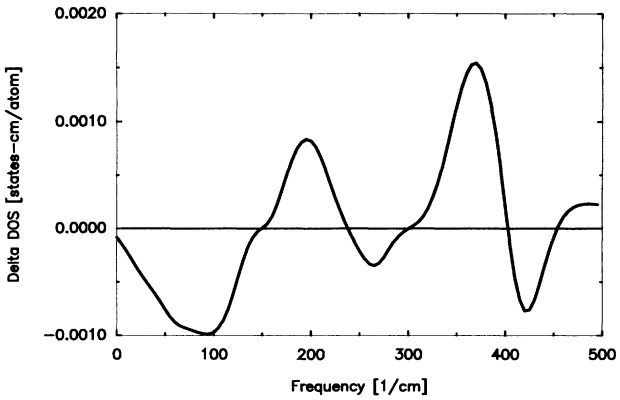

FIG. 14. Difference between the vacancy cell and perfect crystal cell DOS.

$$\Phi_{\mathrm{nnn}}^{0,0,0}=\begin{matrix}0.28 & 0.0 & 0.0\\ 0.0 & 0.29 & 0.0\\ 0.0 & 0.0 & 0.29,\end{matrix}$$

$$\Phi^{1/2,-1/2,0}=\begin{matrix}-0.04 & 0.03 & 0.0\\ 0.03 & -0.04 & 0.0\\ 0.0 & 0.0 & 0.0.\end{matrix}$$

These matrices show the origin of the characteristic spectra: The Einstein frequency along (110) of the atom located at $a_0/2$ (110) is lowered from 300 to 275 cm^{-1}, while the transverse frequency [along $(1-10)$] is increased to 340 cm^{-1}. For second neighbors, both parallel and transverse are increased. The main contribution to these increments is the increased longitudinal spring [0.37 eV/(Å)] for displacements along $(1,-1,0)$ linking atoms at $(1/2,1/2,0)$ and (100), as can be seen from $\Phi^{1/2,-1/2,0}$, compared to its value in the perfect lattice, 10% smaller.

The fact that even at the fourth shell (54 atoms) the influence on the vibrational spectrum is still not negligible, makes that the total DOS of our crystal containing approximately 1% of vacancies is significantly different from the perfect crystal as seen in Fig. 13, and the corresponding difference, ΔDOS, in Fig. 14.

IV. DISCUSSION AND CONCLUSIONS

The solution of Si in the Al matrix increases the free energy of the system driving it into a nonequilibrium state with important consequences on many physical properties. The energy stored in the lattice influences the dynamical behavior as can be deduced from the empirical arguments described in Ref. 19 relating the heat of solution of Si, ΔE_f, the heat of melting of pure Al, L_f, and the Si concentration x to the Debye temperature Θ_D:

$$\Theta_D(\mathrm{Al}_{1-x}\mathrm{Si}_x)=\Theta_D(\mathrm{Al}[1-x(\Delta E_f/L_f)]\ .$$

This expression indicates that when the heat of solution is large compared to the heat of melting, like in the Al-Si case, an instability can be driven for low concentrations of solute.

Our main conclusions are that Si, being smaller than

Al, induces large relaxations and is weakly bonded to its neighbors; it essentially participates in vibrations contained in the lower half of the phonon band, with a local spectrum practically isotropic. Its nn appear to be coupled with a longitudinal spring similar to the perfect lattice case, but the transverse springs are virtually zero. The complex nature of the interactions reflects in the significant hardening of the vibrations involving a particular transverse coupling (curve [001], Fig. 5).

The coupling of Si to its second neighbors is also considerably different, involving a reduction in magnitude and a change in sign. Moreover, the presence of Si affects the Al-Al interactions in its neighborhood: The total restoring forces of Al atoms nn to Si (the diagonal elements of diagonal matrices) reflect complex behavior since, despite the softening of the transverse Al-Si coupling, the total restoring force for motion perpendicular to the Al-Si axis is increased.

The total balance of 1% Si concentration gives an overall drift towards lower frequencies, essentially at the TA peak, and at the high-frequency tail of the LA peak, see Fig. 7. These results are in excellent agreement with experimental observations.

Since these general features are expected to occur in presence of a vacancy as well, we performed similar dynamical analysis for the Al 1% vacancy system. The results show a very similar behavior at the TA peak (compare Figs. 7 and 13), but a marked difference in the LA peak, where the vacancy shows an increase of its height. Vibrations of nn and nnn along directions perpendicular to the vacancy-Al axis are harder than in the perfect crystal and the effect is more pronounced than for Al-Si.

The concentration of modes at high frequency (the LA peak) induced by the vacancy, affects the values of $\langle \omega \rangle$ and $\langle \omega^2 \rangle$ in such a way that a reverse effect is predicted for the superconducting transition (a decrease of T_c as compared to the increase observed for AlSi).

ACKNOWLEDGMENTS

We thank J. Chevrier for valuable discussions and material given prior to publication.

*Present address: Centro Atomico Bariloche, Instituto Balseiro, 8400 San Carlos de Bariloche, Argentina.

[1]W. A. Harrison, Phys. Rev. **136**, A1107 (1966).

[2]W. A. Harrison, in *Pseudopotentials in the Theory of Metals* (Benjamin/Cummings, Menlo Park, CA 1966).

[3]V. Heine and D. Weaire, in *Solid State Physics: Advances in Research and Applications,* edited by H. Ehrenreich (Academic, New York, 1970), Vol. 24, p. 250.

[4]R. Evans and M. W. Finnis, J. Phys. F **6**, 483 (1976).

[5]G. Jacucci, R. Taylor, A. Tenenbaum, and N. van Doan, J. Phys. F **11**, 793 (1981).

[6]C. B. So and C. H. Woo, J. Phys. F **11**, 325 (1981).

[7]M. S. Daw and M. I. Baskes, Phys. Rev. Lett. **50**, 1285 (1983).

[8]M. W. Finnis and J. E. Sinclair, Philos. Mag. **50**, 45 (1984).

[9]S. M. Foiles and M. S. Daw, J. Mater. Res. **2**, 5 (1987).

[10]A. F. Voter and C. P. Chen, in *Characterization of Defects in Materials,* edited by R. W. Siegel, J. R. Weertman, and R. Sinclair, MRS Symposia Proceedings No. 82 (Materials Research Society, Pittsburgh, 1987), p. 175.

[11]V. Vitek, G. J. Ackland, and J. Cserti, in *Alloy Phase Stability and Design,* edited by G. M. Stocks, D. P. Pope, and A. F. Giamei, MRS Symposia Proceedings No. 186 (Materials Research Society, Pittsburgh, 1990), p. 227.

[12]R. Car and M. Parrinello, Phys. Rev. Lett. **55**, 2471 (1985).

[13]O. F. Sankey and D. J. Niklewski, Phys. Rev. B **40**, 3979 (1989); O. F. Sankey, D. A. Drabold, and G. B. Adams, Bull. Am. Phys. Soc. **36**, 924 (1991).

[14]A. Caro, S. Ramos de Debiaggi, and M. Victoria, Phys. Rev. B **41**, 913 (1990).

[15]W. L. Johnson, Prog. Mater. Sci. **30**, 81 (1986).

[16]H. J. Fetch and W. L. Johnson, Nature (London) **334**, 50 (1988).

[17]S. R. Phillpot, S. Yip, and D. Wolf, Comput. Phys. **6**, 20 (1989).

[18]V. F. Degtyraeva, G. V. Chipenko, I. T. Belash, O. I. Barkalov, and E. G. Ponyatowskii, Phys. Status Solidi B **89**, K127 (1985).

[19]J. Chevrier, D. Pavuna, and F. Cyrot-Lackmann, Phys. Rev. B **36**, 9115 (1987).

[20]J. Chevrier, J. B. Suck, J. J. Capponi, and M. Perroux, Phys. Rev. Lett. **61**, 554 (1988).

[21]J. Chevrier, J. C. Pasjaunias, F. Zougmore, and J. J. Capponi, Europhys. Lett. **8**, 173 (1989).

[22]J. Chevrier, J. B. Suck, J. C. Lasjaunias, M. Perroux, and J. J. Capponi, Phys. Rev. B **49**, 961 (1994).

[23]E. A. Stern and K. Zhang, Phys. Rev. Lett. **60**, 1872 (1988).

[24]H. Shechter, E. A. Stern, Y. Yacoby, R. Brener, and Z. Zhang, Phys. Rev. Lett. **63**, 1400 (1989).

[25]G. B. Adams and O. F. Sankey, Phys. Rev. Lett. **67**, 867 (1991); D. A. Drabold, P. A. Fedders, S. Klemm, and O. F. Sankey, *ibid.* **67**, 2179 (1991); D. A. Drabold, R. Wang, S. Klemm, and O. F. Sankey, Phys. Rev. B **43**, 5132 (1991); S. H. Yang, D. A. Drabold, J. B. Adams, and A. Sachdev, *ibid.* **47**, 1567 (1993).

[26]D. R. Hamann, M. Schlüter, and C. Chiang, Phys. Rev. Lett. **43**, 1494 (1979).

[27]J. Harris, Phys. Rev. B **31**, 1770 (1985).

[28]D. M. Ceperley and G. J. Alder, Phys. Rev. Lett. **45**, 566 (1980).

[29]J. Perdew and A. Zunger, Phys. Rev. B **23**, 5048 (1981).

[30]P. H. Dederich and R. Zeller, in *Point Defects in Metals II,* edited by G. Höhler, Springer Tracts in Modern Physics Vol. 87 (Springer-Verlag, Berlin, 1980), p. 67.

[31]F. Ercolessi and J. Adams (unpublished).

[32]W. L. McMillan, Phys. Rev. B **167**, 331 (1968).

[33]M. J. Guillan, J. Phys.: Condens. Matter **1**, 689 (1989).

[34]R. W. Jansen and B. M. Klein, J. Phys.: Condens. Matter **1**, 8359 (1989).

[35]M. J. Mehl and B. M. Klein, Physica B **172**, 211 (1991).

[36]R. Benedek, L. H. Yang, C. Woodward, and B. I. Min, Phys. Rev. B **45**, 2607 (1992).

[37]R. D. Hatcher, R. Zeller, and P. H. Dederich, Phys. Rev. B **19**, 5083 (1979).